Verification of positional tolerances with a 3D non-contact measurement method

R. Minguez [(a)], A. Arias [(a)], O. Etxaniz [(a)], E. Solaberrieta [(a)], L. Barrenetxea [(a)], A. Olano [(a)]

[(a)] Product Design Laboratory, Faculty of Engineering of Bilbao (The University of the Basque Country, UPV/EHU)

Abstract

Purpose:
New methods of data acquisition such as 3D scanners have become increasingly necessary for the verification of the geometric dimensioning and tolerancing (GD&T) specifications in the manufacture of industrial parts.

Method:
This paper proposes a method for the verification of a positional tolerance in two cylindrical features in an industrial part digitized using a 3D non-contact scanner. Apart from a method that permits an adequate quantification of the obtained results, different ways of visualizing the results are displayed throughout this article.

Result:
The tolerance zone within which the used scanner carries out the analysis was measured and quantified. Some aspects taken into consideration were the geometric quality of the piece and the repeatability, reproducibility and uncertainty of the digital process, which comprises the acquisition and processing of the data.

Discussion & Conclusion:
This research work concludes that the digital method presented hereby, with its corresponding virtual inspection, is valid for the verification of positional tolerances, even when it is required that the GD&T specification are maintained regardless of the features' actual mating envelope size.
In addition, this article raises the debate over the best way to adapt the traditional datum referencing rules to the new data acquisition methods.

1 Introduction

In the industrial practice, position tolerance is the most frequently used geometric tolerancing characteristic and the verification of this and another manufacturing geometric dimensioning and tolerancing (GD&T) specifications in man-made engineering parts with traditional contact measurement and fixture methods is a long studied issue [1], [2], [3].

The fast development of Geometrical Reverse Engineering techniques by means of the 3D optical scanners allows that non-contact measurement methods can be compared with the contact measurement methods [4], [5], [6], [7].

Besides there is an ever-increasing industrial demand for measurements in medium and large sized engineering parts, which can take days if carried out using traditional contact methods or specifically designed go/no go gauge devices.

For this reason, a direct comparison between the proposed non-contact measurement method through a 3D optical scanner and the traditional method, performed with a Coordinate Measure Machine (CMM), was carried out in order to verify the positional tolerance of two cylindrical holes of a piece.

Within the group of tolerances denominated tolerances of location, a positional tolerance defines the total permissible variation in the location of a feature from its true position. In the studied case, with a cylindrical feature, this total permissible variation will be the diameter of the cylindrical zone in which the axis or the centre of the feature deviated from its theoretically exact position can be found [8].
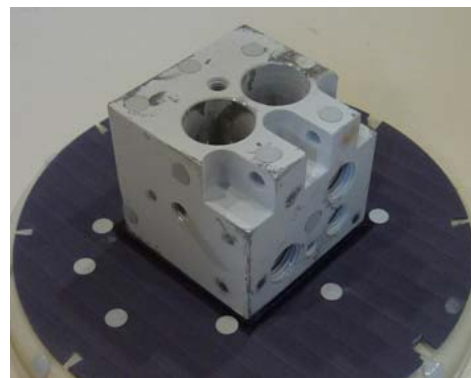

Fig. 1 Sample part.

Therefore, the main objective of this paper is to propose a method for the verification of a positional tolerance by means of the verification of the geometric tolerance of two cylindrical holes of diameter 19 mm. This verification will be implemented on the body of fig. 1.

2 Used models and proposed verification method

It is assumed that the part complies with the manufacturing specifications contained in the engineering drawing in fig. 2. The position of the axis of the two holes will be controlled with a positional tolerance without taking into account the real dimensions of the manufactured piece. The geometric tolerance is applied on an RFS basis. Each hole must be located within the specified positional tolerance regardless of the size of that hole. The positional tolerance applied at RFS is more restrictive than the same positional tolerance applied at MMC (or LMC) [9].
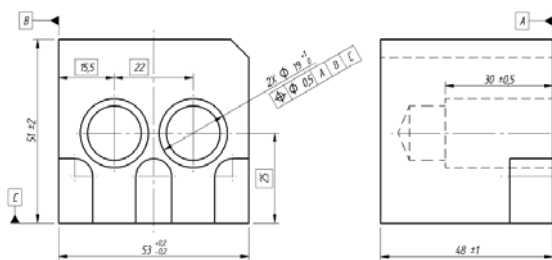

Fig. 2 Drawing of the model (RFS).

2.1 Proposed verification method

The way of processing and interpreting the data obtained with the non-contact measurement method will be processed and analyzed to verify whether the part under study accomplishes the desired positional tolerancing or not. The data provided by a CNC Coordinates Measurement Machine (CMM) will be used as true measures. The CMM will be a Mitutoyo BH-504 ™ (Mitutoyo Corporation, Japan) with an accuracy give by the manufacturer of 0.003 mm and a given precision under ±0.001 mm (2σ).

The method used to verify this tolerancing will consist in analyzing a collection of scanning sessions of the studied part and then, the tolerances of the referred cylindrical zones through the assumptions of the first model and the second model will be checked. The scanning device will be an ATOS Compact Scan 5M™ (GOM GmbH, Germany) with an accuracy give by the manufacturer of 0.010 mm and an studied precision [10] under ±0.05 mm (2σ).

This verification will be carried out through a virtual, ideal, go-no go gauge device [11], designed with a CAD program [12], where it can be easily tested whether the scanned part complies or not with the tolerance established for their holes.

This gauge element is a piece specifically designed for the validation of the proposed case. Its design must permit adjusting the part according to the plane specifications and in addition, it must enable a direct 3D or 2D visualization to verify the conformity of the analyzed tolerance with the standard.

Therefore, a comparison between the gauge piece and the scanned data will quickly determine whether or not the piece meets the required tolerances.

Fig. 3 shows the gauge piece associated with the model, which must meet the RFS basis. The two small cylinders represent the tolerance zone and the three inner faces represent the datum planes A, B and C.
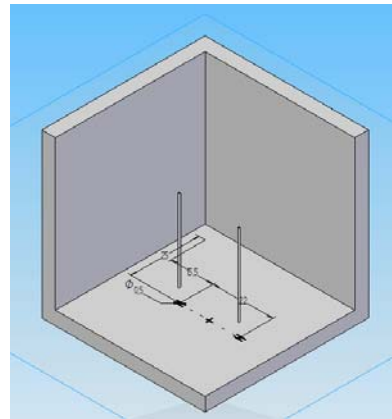

Fig. 3 Virtual gauge for the virtual model.

To guarantee the validity of the selected method, all results obtained across different tests must be within a restrictive acceptable range.

Three collections or series of eight different scan sessions will be taken on the RFS basis, in such a way that for the used scanner it can be verified that the results are the same regardless of the collection and of the number of scan session within the collection.

All scans carried out were subsequently processed through the program Geomagic Studio 2012 ™ (Geomagic, Inc., NC, USA). This program is specifically designed for the edition, processing and analysis of point clouds and triangular meshes. Taking into account the repeatability and reproducibility of the measurements, the method must be independent of the technician, the scanner device and the scanning session. In all cases the same sequence of operations will be performed to check whether the tolerance of the piece falls or not within the specified limits.

The proposed method consists in adjusting the acquired data, in the form of a point cloud or mesh, to the element used as datum feature simulator in the best possible way according to the existing ASME Y14.5-2009 standard.

This standard prioritizes certain planes over the rest. It also establishes how to carry out the adjustments necessary for the correct definition of a positional tolerance. Obviously, this should be the method used to adjust planes A, B and C of the studied part against the virtual gauge.

Following the standard, the CMM alignment should be replicated. Hence, a 3-2-1 alignment would be performed using specific features (plane, vector and origin point) extracted from the mesh [13]. In the case of the studied models, the order in the adjustment of the datum planes will be A, B and C. Thus the piece will be supported first by plane A, then, it will contact plane B and finally, it will reach plane C.

However, when applying the standard directly to a STL file obtained directly from the 3D digitizer, the adjustment of these planes is inevitably affected by some aspects such as noise in the scanned part, the area of the targets used for referencing in the scanning session, and some small irregularities in the arrangement of the triangles to create the STL file [14], [15], [16].

The ASME standard was created for physical pieces resting on real datum features. Section 5 will show that if this standard were strictly followed, the results would be different.

Taking into account these facts, it was decided that the fixture setting made by the program used for comparison

would be used in this tolerance measurement, so the standard would have to be adapted to the data obtained with the 3D scanner.

Some fitting operations were performed on the three indicated planes, giving greater importance to plane A, in such a way that the interpolated plane A, obtained from the STL, coincides with the theoretical one. A secondary importance was given to the interpolated plane B, which will present a small error in the adjustment. The interpolated plane C was given a minimum importance. Therefore, it will present the biggest error.

Using this type of adjustments with the datum planes ensures that the fitting of the tolerance will not affect a subsequent analysis with the aforementioned problems arising from a scanned file, such as the noise in the STL file or even the area of the circular references used during data collection.

2.2   *Results of the tolerancing verification*

Since the proposed verification method was used in each conducted session, the results from any of them are directly comparable.

Fig. 4 presents a comparison between the results obtained in the study case. The figure clearly shows whether the studied feature is located or not within the established parameters of tolerance.

When the RFS basis is applied, the axis of the scanned characteristic (the cylindrical feature) is made to appear in the drawing. In this case, the axis must remain within the tolerance zone of the gauge element (Fig. 3).

Consequently, a section was practiced on each of the two tolerance cylinders of the gauge piece in such a way that in a cross-section view, the interpolated axis will be displayed in true magnitude. Fig. 4 shows the section made on the two cylinders, as well as the interpolated axes. It confirms that both axes remain within the tolerated area.
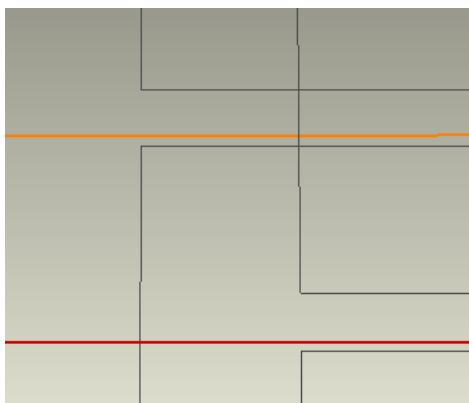

Fig. 4 Comparison when RFS basis is applied.

This comparison was carried out with all the conducted scanning sessions. The results obtained proved to be clearly similar, but hardly quantifiable.

For this reason, it can be affirmed that on the one hand, this approach based on the principle of virtual go-no go gauge devices is a valid inspection method to confirm whether a piece is or not within set tolerances. But on the other, following the ASME standard, it cannot determine how much the piece deviates from the theoretical value.

This method is a fast and reliable way to control large sets of pieces. It permits a quickly and reliable analysis

and it makes the decision on the validity or not of a piece a simple task easily achievable by anyone.

3   Quantification method

The next point of the article aims at quantifying what so far has only visually displayed. To achieve this quantification, it was decided to extract the coordinates from the axis numerically. This new approach will result in an analysis that will differ from the previous ones.

The way to extract the coordinates of a number of points in the axis defined by the point clouds processing program will first be explained.

The extraction of the coordinates of a point of the axis is part of the analysis carried out earlier. After completing the analysis, the axes of both cylinders, together with the main plane A, wherever they are defined, must be exported to an IGS file.

The IGS file will be opened later with a 3D design program (Solid Edge ST4, Siemens PLM Software, Germany) used for the creation of the virtual gauge elements. In fig. 10, only two of the axes are displayed because in this case, the exported plane A corresponds to the x-y plane.

Although theoretical planes B and C were not exported, as the gauge element was modelled out with the same program, these planes will correspond to the planes x-z and y-z respectively.

Once the IGS file is opened, a plane parallel to the datum plane A should be defined. Then, as fig. 5 shows, the coordinates of the intersection with the axis will be measured in the two planes.
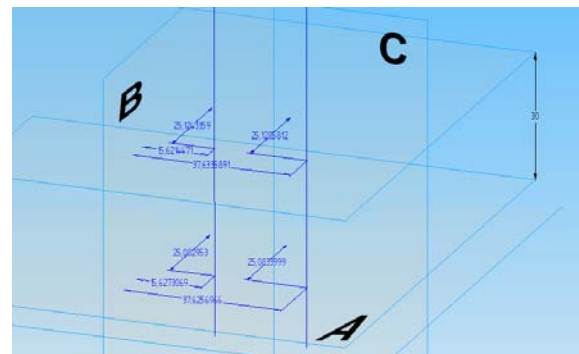

Fig. 5 Axes exported to the CAD program and fixed to the

virtual gauge element.

This procedure will be completed with each of the 8 scan sessions of the 3 collections that were carried out. This will result in a table of numeric data from the interpolated axes from the point cloud.

Before addressing the resulting tables directly, it is certainly convenient to go over the methodology as well as the formulation used to analyze the data from the tables.

The main concept lies on the fact that any axis that can be extracted from the scanned data belongs to a cylinder with its radius determined by the positional tolerancing and its axis perpendicular to the theoretical plane A.

In this study, as the axis is limited to the scanned depth of the hole, so the maximum possible length of the cylinder is 30 mm.

Following this model, it can be stated that the points of the axis at level 0 mm and at level 30 mm will be the only points of the axis that will be in contact with the walls of

the theoretical cylinder that comprises the real axis. Therefore, in a view perpendicular to plane A, the points registered at levels 0 mm and 30 mm will be two points of the same circle that will define the diameter of the tolerance cylinder.

This concept is subsequently applied to each of the scanning sessions. A few sets of points corresponding to heights 0 mm and 30 mm will be obtained. They will be used for the correct definition of a cylinder, covering all the axes generated during these different scanning collections.

3.1 Mathematical definition of the tolerance zone

This point will explain how to define mathematically the circles that determine the tolerance zone. Later on, the results obtained following this methodology will be displayed.

The definition of a circle in a spreadsheet application requires knowing the centre of the circle, with its coordinates (xc, yc), as well as its radius R.

Once this data is obtained, two rows will be generated. Each of them will include fifty values, corresponding to different points on the circle. These rows will be generated according to the following formulas, which are designed to represent a point on a circle each 7.5° of rotation (eq. 1, eq. 2).

$$x_i = x_c + R\cos\left(\frac{i*\pi}{25}\right) \qquad i = 1,...,50 \qquad (1)$$

$$y_i = y_c + R\sin\left(\frac{i*\pi}{25}\right) \qquad i = 1,...,50 \qquad (2)$$

The first step will thus consist in defining correctly a circle that contains a number of points within. In this case, the previously obtained coordinates from the scanning sessions will be used.
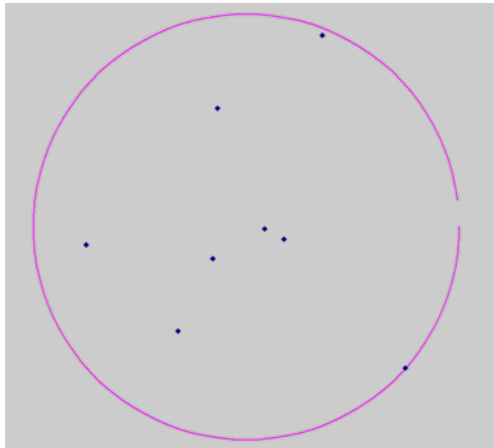

Fig. 6 Circle covering points at 30 mm level from the first scanning collection.

As fig. 6 shows, the starting data are a number of points that have the coordinates (xᵢ, yᵢ) and are intended to generate a circle that includes all of them. This circle is not the circle circumscribed to the points, but the circle the centre of which has the arithmetic average value of the points. In this way, the resulting circle considers these data from a statistical point of view.

The coordinates of the midpoint of the circle are defined by eq. 3 and eq.4.

$$x_c = \frac{\sum_{i=0}^n x_i}{n} \qquad (3)$$

$$x_c = \frac{\sum_{i=0}^n x_i}{n} \qquad (4)$$

Alternatively, to define the radius of this circle, the distance that separates the most distant point from the above-defined centre was chosen. This ensures that all points in the interior of the circle are covered (eq. 5).

$$R = \max\left(\sqrt[2]{(x_i - x_c)^2 + (y_i - y_c)^2}\right) \qquad i = 1,...,n \qquad (5)$$

At this point, as it has been previously explained, a global circle covering the points can be generated. In this case, this circle includes a set of points that can correspond to either the 0 mm level or the 30 mm level, but never combined points. This step aims at extrapolating the above-explained idea of an axis to a set of axes.

Therefore, when following this method, two different circles will be obtained. One circle will correspond to the data collected at 0 mm level data and the other, to the data collected at 30 mm level.

The next step of this method requires the definition of a circle tangent to the previously defined two circles. This circle will represent the projection of the cylinder including all analyzed axes.

Having these two circles, the third circle containing them and at the same time, being tangent to them is generated. Fig. 8 shows the three circles, where the third circle tangent to the other two can be observed.

The first step in the calculation of the aforementioned circle is the definition of its radio. Being R₁ the radius of the top circle and R₂ the radius of the lower circle, and being (x₁, y₁) the centre of the upper circle and (x₂, y₂) the centre on the bottom, the radio is defined in eq. 6.

$$R = \frac{\sqrt[2]{(x_1 - x_2)^2 + (y_1 - y_2)^2} + R_1 + R_2}{2} \qquad (6)$$

Then, the angle α must be obtained, as shown in fig. 7, through the formulation in eq. 7.

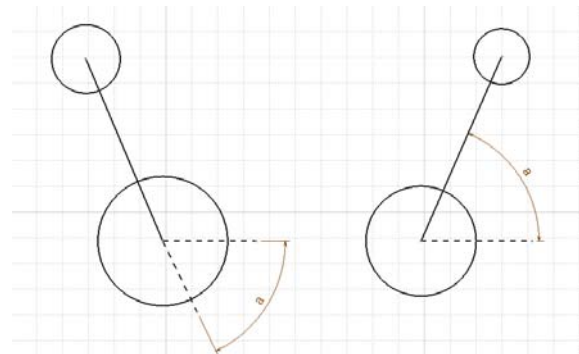$$\propto = arctg\left(\frac{y_1 - y_2}{x_1 - x_2}\right) \qquad (7)$$

Fig. 7 Two cases when obtaining the angle α.

The next step consists in defining the two points of tangency with the two smaller circles that this third circle must have. The resolution will be performed in a spreadsheet application and, depending on the position of the initial circle centre, the resolution will present two differentiated cases.

This is due to the spreadsheet application, which calculates the angle α of the line connecting the centres of the two initial circles as a different angle depending on

how the centres of these circles are positioned. The first case is applicable when $x_1 < x_2$ as noted in fig. 9 and in fig. 7 on the right side (eq. 8, eq. 9).

$$x_a = x_1 + R_1 \cos \alpha \qquad y_a = y_1 + R_1 \sin \alpha \qquad (8)$$

$$x_b = x_2 - R_2 \cos \alpha \qquad y_b = y_2 - R_2 \sin \alpha \qquad (9)$$

The second case is applicable when x1>x2 as noted in fig. 8 and in fig. 7 on the left side (eq. 10, eq. 11).

$$x_a = x_1 - R_1 \cos \alpha \qquad y_a = y_1 - R_1 \sin \alpha \qquad (10)$$

$$x_b = x_2 + R_2 \cos \alpha \qquad y_b = y_2 + R_2 \sin \alpha \qquad (11)$$

Once the tangency points are defined, as indicated in eq. 12 and eq. 13, there will be sufficient data to define the centre of the tangent circle.

$$x_c = \frac{x_a + x_b}{2} \qquad (12)$$

$$y_c = \frac{y_a + y_b}{2} \qquad (13)$$

Having the circle defined and knowing its radius R, the circle can be then defined in the spreadsheet application as explained before.

The results displayed in figs. 8 and 9 are the results obtained and quantified following the explained methodology.
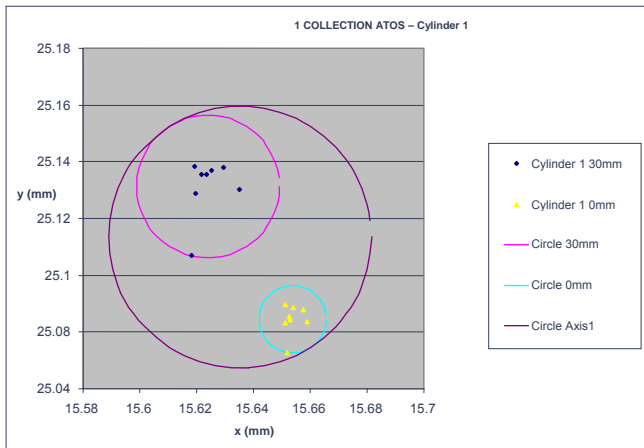

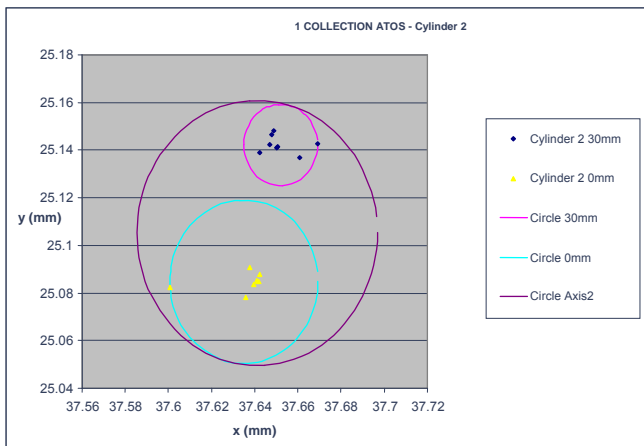**Fig. 8 Tolerance zone for the first cylindrical feature.**

Fig. 9 Tolerance zone for the second cylindrical feature.

The third circle shown in the graph is tangent to the previous two and shows the possible positions that could deal with the axis of the cylinder scanned on different occasions, bounded in a range from the 0 mm level to the 30 mm level.

The data to compute the greater circles are the following:
- Cylinder 1: R_1 = 0.046 mm; C_1 (15.635; 25.113)
- Cylinder 2: R_2 = 0.056 mm; C_2 (37.641; 25.105)

3.2   Conclusions (of the quantification method)

From the data displayed in fig. 8, it can be concluded that the used scanner was able to group the points measured at 0 mm level in a diameter of 0.024 mm, for the eight cases scanned in the first sequence (blue circle).

In contrast, the 30 mm level presents a higher scattering in its points and they are grouped in a circle of diameter 0.050 mm (pink circle).

It can be thus concluded that the axis of cylinder 1 is confined in a cylinder of diameter 0.092 mm between 0 mm level and 30 mm level, represented by the greater circle.

As in the previous case, according to fig. 9, the conclusion to be drawn is that the ATOS Compact Scan 5M ™ (GOM GmbH, Germany) scanner was capable of grouping the points of the second cylinder measured at 0 mm level in a diameter of 0.069 mm, blue circle, for the eight cases scanned in the first sequence. In this case, the radio is greater mainly due to the first point of the sequence, which differs considerably from the rest.

On the other hand, the 30 mm level presents a greater scattering of its points in general but in this case, because the first item in the series is at 0 level, all the points at this level are grouped in one circle smaller than the previous one of diameter 0.034 mm (pink circle).

Therefore, the axis of cylinder 2 is confined in a cylinder of diameter 0.111 mm between levels 0 mm and 30 mm, represented by the purple circle.

This procedure was followed for the other two remaining scanning collections with similar results, and therefore the graphs obtained in these cases will not be displayed.

4   Comparison with the CMM

The used part is not a calibrated piece, so it was considered convenient to extract more information from the three completed sample collections by comparing them also with the measurements obtained with the coordinate measurement machine. These measurements can be considered as true measurements due to the accuracy range of the CMM. As it is well known, factors like the calibration of the equipment and the ambient temperature affect the measurements made with the optical device. However, the results obtained from this comparison clearly show that the data obtained without contact do not differ significantly from the points obtained through a CMM.

The concept used to define the following graphs is exactly the same as the concept used up to this moment, but with a greater number of points. The circle containing the axis measured by the used CMM is also included in the graph, so it can be a way of comparing these two methods of verification of tolerances: with and without contact (figs. 10 and 11).
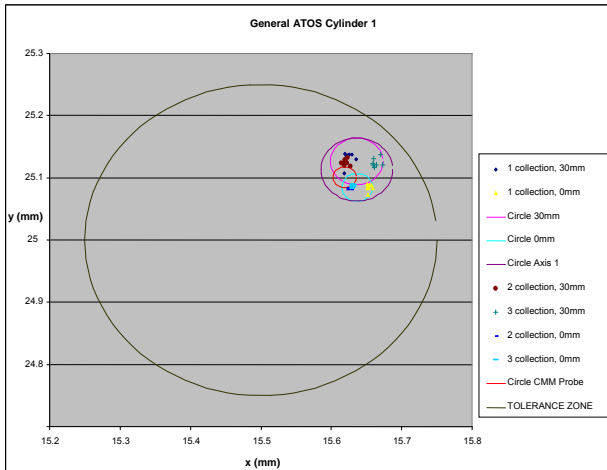
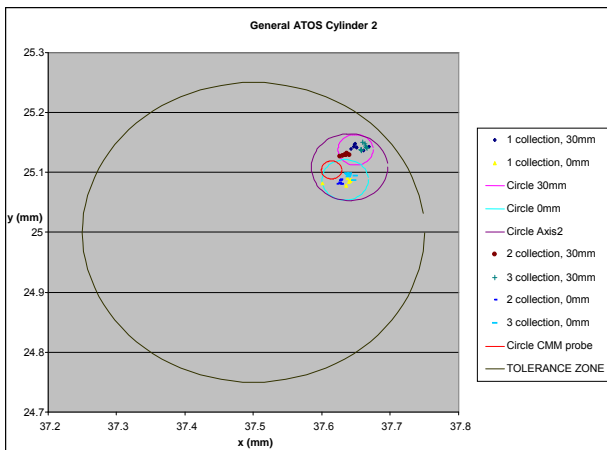**Fig. 10 Tolerance zones for the first cylindrical feature.**

Fig. 11 Tolerance zones for the second cylindrical feature.

The graphs on figs. 10 and 11 clearly represent that the uncertainty area bounded for the cylinder of tolerance obtained by means of digitalization is greater than the area that represents the cylinder of tolerance measured by the CMM, as this circle is included within the area bounded by the values obtained from scanning. Therefore, the measure may always be considered appropriate and its range of uncertainty permitted.

For the specific case discussed in this paper, the measure given by the 3D scanner is valid, because all the area bounded by the larger cylinder lies within the tolerance area defined by the positional tolerance applied on a RFS basis.

5   Conversion to standard ASME Y14 practices

The measurement validation methodology should go one more step forward. The next action that was carried out consisted in comparing the adjustment made by the processing program of the point cloud, with the adjustments should be carried out according to the practices indicated in standards ASME Y 14.5-2009 [9] and ASME Y 14.43-2011 [17].

As explained before, the calculation of the datum planes is affected by the program algorithms and the noise in the mesh, while ASME standard was created for physical pieces resting on real datum features.

In order to perform this comparison between the standard practices and the adjustments introduced by the methodology followed in this article, the position of one point of each axis must be corrected. To perform this correction, the points that define the positions of the axes measured with the contact probe were chosen. This modification was calculated quantifying the difference in the adjustment of the two procedures that are going to be compared.

The first computation that fits directly the extrapolated datum planes of the point cloud to the datum planes of the virtual gauge piece is changed to the CMM alignment, commonly named 3-2-1 alignment, that can be also applied by the reverse engineering program.

Once the position of these axes is corrected, the coordinates (x, y) of the different points corresponding to the cut of each axis with the two used planes at 0 mm level and 30 mm level are obtained.

This enables a comparison between both forms of adjustment, which allows displacing centres of the obtained circles for the different axes based on the retrieved displacement computed with the theoretical axis measured with a CMM.

Fig. 12 shows the displacement afflicting the axis according to the adjustment made through the program (Geomagic Studio 2012 ™, Geomagic, Inc., NC, USA) to edit the point clouds and through the method indicated in standard ASME Y14.

An analysis of these data concludes that the displacement of axes 1 and 2 will be defined as the difference between the value obtained by the default option in the point cloud processing program and the value obtained by application of the adjustment in the Standards ASME Y14 in the processing program.

Cylinder 1

	Geomagic	ASME Y14	Displacement
X value	15.619	15.655	0.036
Y value	25.101	25.356	0.255

Cylinder 2

	Geomagic	ASME Y14	Displacement
X value	37.614	37.664	0.050
Y value	25.103	25.360	0.257

Fig. 12 Values of the displacement for the two cylindrical features.

Finally, the obtained displacement for each of the axes was applied to the calculated tolerance circle of the global scanned data, achieving in this way the position of the scanned axis regarding the standard ASME Y14.5 practice. Figs. 13 and 14 illustrate the comparison between both methods of adjustment.
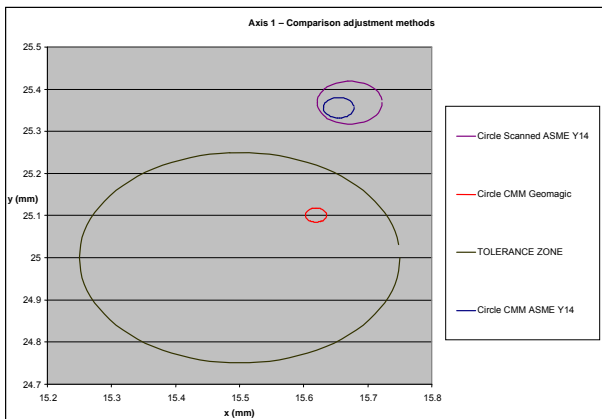
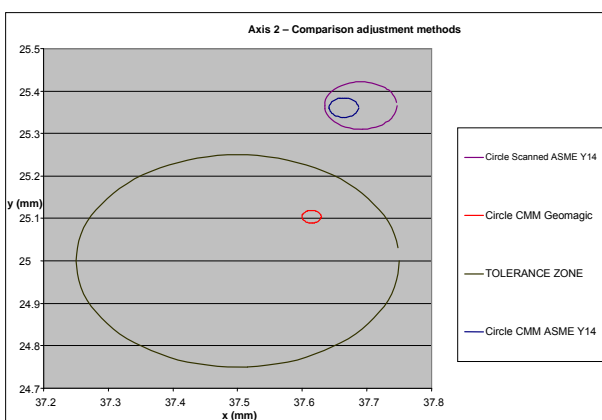**Fig. 13 Cyl. 1. Comparison between adjustment methods.**

Fig. 14 Cyl 2. Comparison between adjustment methods.

6   Conclusion and discussion

Considering the information extracted from all the previous graphs, it can be concluded that using the scanned point clouds, the processing program and the virtual gauge device according to the adjustment indicated by the standards ASME Y14.5, the studied part is not within the manufacturing tolerances indicated in the plane.

Besides, it can be pointed out that the existing displacement between both settings can be defined, thanks to which it was accurately quantified.

Therefore, it can be concluded that although the results obtained by the processing of the point clouds by the program do not conform perfectly to the standard, they can be adapted to this standard when required.

In addition, this article raises the discussion on the need to approve either a new regulation, or an adaptation of the existing standard that adjusts to the new technologies of data collection. It cannot be ignored that when processing an amount of information much greater than the obtained with traditional methodologies, the framework for which such a standard was drafted may be exceeded [18].

At present, the amount of points obtained with a 3D optical scanner is so vast that an interpolation of the scanned points corresponding to the datum planes and the subsequent overlapping on the datum planes in the virtual gauge device seems more correct than trying to adapt the cloud of points to the gauge by means of the 3-

2-1 standard adjustment in which planes with a much smaller amount of points can be easily fitted.

The method used to measure the positional tolerance by means of the processing of the point cloud is very precise with a high ability to repeat and reproduce the results, although the real position of the axis remains highly uncertain due to the unknown accuracy of the algorithm to compute de datum planes used by de processing program.

The conclusion reached in this article is that the used scanner can perform measurements with a range of uncertainty that can be considered accurate, bounded in a circle of radius 0.0375 mm.

But on the other hand, according to the adjustment method, the difference in the setting of the second axis is 0.262 mm in absolute value for the studied part. Taking into account that the indicated tolerance is 0.5 mm, this is a significant difference.

This difference is mainly due to the displacement in the y axis. Fig. 15 illustrates the angles between all planes and shows that plane C presents the worst perpendicularity with respect to the other two planes. This error is certainly reinforced by the adjustment method of the reverse engineering program.
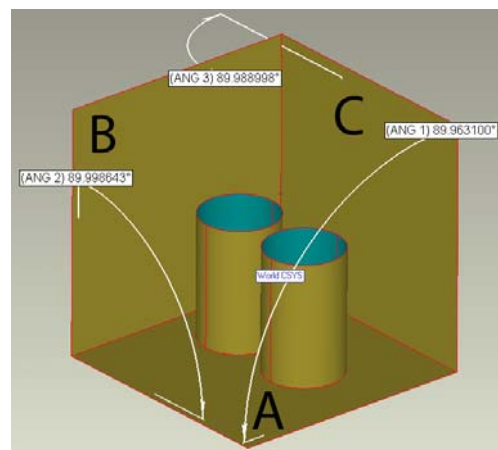

Fig. 15 Angles between the scanned target angles.

From this article, it can be concluded that a 3D non-contact measurement is valid to quantify a position tolerance zone when the range of the geometrical tolerance does not require higher precision than the scanner's range of uncertainty, being its greatest advantage over CMM machines the important fact that it can be easily transported to the place where the measurement must be carried out. The move from 'go-no go' based gauge device inspection to a digital gauge inspection and a product life cycle environment should significantly reduce the cost of new inspections.

Acknowledgement

References

[1]   E. R. Evans. Solid Models, Virtual Inspection and the Position Tolerance.

Proc. of the 59th Annual Midyear Meeting, 2004, ASEE, Williamsburg, Virginia, USA, pp 153-158.

[2] S. A. Tahan, S. Levesque. Exploiting the process capability of position geometric tolerance according GD&T ASME Y14.5M. International Conference on Computers and Industrial Engineering CIE 2009, 2009, pp 1297-1272.

[3] R. J. Urbanic, W. ElMaraghy, H. ElMaraghy. An integrated systematic design recovery framework. Journal of Computing and Information Science in Engineering 6 (2006) pp 318-330.

[4] M. Germani, P. Corbo, F. Mandorli. A cad based tool for automatic control of geometrical tolerances. Proc. of the XVII Ingegraf and XV ADM International Congress, (2006) Seville, Spain.

[5] G. Lukacs, J. Lockhart, M. Facello. Non-contact whole-part inspection. http://www.geomagic.com/download_file/view/1872/5764. (2012) Accessed 10 January 2013.

[6] H. Pottmann, S. Leopoldseder, M. Hofer, T. Steiner, W. Wang. Industrial geometry: recent advances and applications in CAD. Computer-Aided Design 37, 2005, pp 751-766.

[7] T. Várady, R. Martin, J. Cox. Reverse Engineering of Geometric Models – an introduction. Computer-Aided Design 29, 1997, pp 255-268.

[8] G. Kaisarlis, S. Diplaris, M. Sfantsikopoulos. Geometrical position tolerance assignment in reverse engineering. International Journal of Computer Integrated Manufacturing 21, 2008, pp 89-96.

[9] ASME Y14.5-2009, "Dimensioning and Tolerancing".

[10] B. R. Barbero, E. S. Ureta. Comparative study of different digitization techniques and their accuracy. Computer-Aided Design 43, 2011, pp. 188-206.

[11] E. Pairel. Three-dimensional metrology with the virtual fitting gauges. Proc. of the 11th CIRP International Conference on Computer Aided Tolerancing, (2009) Annecy, France.

[12] M. Germani, F. Mandorli, M. Mengoni, R. Raffaeli. CAD-based environment to bridge the gap between product design and tolerance control. Precision Engineering 34, 2010, pp 7–15.

[13] F. Concas. Design of Optimal Measurement Strategies for Geometric tolerances Control on Coordinates Measuring Machines. PhD Thesis (2006) Universitá degli Studi di Calgliari.

[14] L. Pino, F. Bennis, C. Fortin. The use of a kinematic model to analyze positional tolerances in assemblies. Proc of the 1999 IEEE International Conference on Robotics & Automation, (1999) Detroit, Michigan, USA.

[15] T. Várady, M. Facello, Z. Terék. Automatic extraction of surface structures in digital shape reconstruction. Computer-Aided Design 39, 2007, pp 379–388.

[16] V. Weiss, L. Andor, G. Renner, T. Várady. Advanced surface fitting techniques. Computer Aided Geometric Design 19, 2002, pp 19-42.

[17] ASME Y14.43-2011, "Dimensioning and Tolerancing, Principles for Gages and Fixtures".

[18] V. Srinivasan. Standardizing the specification, verification, and exchange of product geometry: Research, status and trends. Computer-Aided Design 40, 2008, pp. 738–749.